

SHEAR AND FLEXURAL STRENGTHENING OF R/C BEAMS WITH CARBON FIBER SHEETS

By Tom Norris,¹ Hamid Saadatmanesh,² Member, ASCE,
and Mohammad R. Ehsani,³ Member, ASCE

ABSTRACT: The results of an experimental and analytical study of the behavior of damaged or understrength concrete beams retrofitted with thin carbon fiber reinforced plastic (CFRP) sheets are presented. The CFRP sheets are epoxy bonded to the tension face and web of concrete beams to enhance their flexural and shear strengths. The effect of CFRP sheets on strength and stiffness of the beams is considered for various orientations of the fibers with respect to the axis of the beam. Nineteen beams were fabricated, loaded beyond concrete cracking strength, and retrofitted with three different CFRP systems. The beams were subsequently loaded to failure. Different modes of failure and gain in the ultimate strength were observed, depending on the orientation of the fibers.

INTRODUCTION

As documented in the eleventh report of the Secretary of Transportation to the Congress of the United States on "Highway Bridge Replacement and Rehabilitation Program," over one third of the nation's 575,413 inventoried highway bridges are classified as either structurally deficient or functionally obsolete (FHA 1993). Deficiencies are usually the result of deterioration caused by age and exposure to adverse environments, heavier traffic brought about by a growing society, or functional changes such as higher required permit load. As a result, a large number of concrete highway bridges are in need of rehabilitation or replacement.

Historically, concrete members have been repaired by post-tensioning or jacketing with new concrete in conjunction with a surface adhesive (Klaiber et al. 1987). Since the mid 1960's, epoxy bonded steel plates have been used in Europe and South Africa to retrofit flexural members (Dussek 1987). Steel plates have a durability problem unique to this application, because corrosion may occur along the adhesive interface. This type of corrosion adversely affects the bond at the steel plate/concrete interface and is difficult to monitor during routine inspections. Additionally, special equipment is necessary to install the heavy plates. As a result of these problems, alternative materials have been sought by engineers.

This paper discusses the use of flexible carbon fiber sheets wrapped around the web and tension flange of reinforced concrete beams to increase their shear and flexural strengths. These sheets are made from high-strength carbon fibers placed in a resin matrix. Since the carbon/epoxy composite system is not affected by electrochemical corrosion, the corrosion problem at the interface encountered in the steel plate bonding is eliminated.

Many researchers have studied the mechanical properties of advanced fiber reinforced composites. However, relatively few studies have been conducted on the combination of fiber composites and traditional construction materials as a way of improving the behavior of civil engineering structures.

Triantafyllou and Plevris (1991) devised analytical models

for the various failure modes of composite beams. Uji (1992) examined continuous fiber sheets applied as shear reinforcement for concrete beams. An et al. (1991) provided a parametric study to predict the behavior of composite beams plated for flexural reinforcing.

Several experimental studies have also been performed to verify existing analytical work or pilot studies. Saadatmanesh and Ehsani (1990, 1991) have conducted studies with glass fiber reinforced plastic (GFRP) plates bonded to the tension flange of concrete beams. Meier and Kaiser (1991) have performed similar studies using carbon plates. Dolan et al. (1993) epoxy bonded a Kevlar fabric wrap to prestressed concrete beams and evaluated its effect on shear capacity. Ritchie et al. (1990) built a series of beams at Lehigh University, Bethlehem, Pa., reinforced them with various types of fiber reinforced plastic (FRP) or steel plates, and tested them to failure. Rostasy et al. (1991) tested the interface shear strength of bonded carbon fiber plates and applied the results for retrofitting of a box girder bridge in Germany. In Japan, concrete beams strengthened with FRP were studied by Sakai et al. (1992).

In this study, nineteen understrength reinforced concrete beams were built, retrofitted and tested to failure. Most of the beams were precracked prior to retrofitting to more closely represent the field conditions. Increases in strength of 20%–100% over the control, unretrofitted beams were noted. The measured results were compared with predicted values obtained from a computer program developed to predict the load-displacement response to failure. The agreement between the measured and predicted values was reasonably good.

FIBER REINFORCED PLASTICS (FRP)

FRPs are used in the aerospace and automotive fields because of their high strength to weight ratio, durability, and ability to form complex shapes. They are generally constructed of high performance fibers such as carbon, aramid, or glass which are placed in a resin matrix. By selecting among the many available fibers, geometries and polymers, the mechanical and durability properties can be tailored for a particular application. This synthetic quality makes FRP a good choice for civil engineering applications as well.

Carbon fibers have a high elastic modulus and high strength in both tension and compression, and are utilized in this study. Composed almost entirely of carbon atoms, the fibers are generally available as bundles of 500–150,000 filaments of approximately five microns in diameter called "yarn." These are then assembled directly into FRP products or into intermediate forms such as continuous fiber sheets or fabrics. Continuous fiber sheets are made of parallel yarns attached to a flexible

¹Res. Asst., Federal Hwy. Admin., McLean, VA 22101.

²Assoc. Prof., Dept. of Civ. Engrg. and Engrg. Mech., Univ. of Arizona, Tucson, AZ 85721.

³Prof., Dept. of Civ. Engrg. and Engrg. Mech., Univ. of Arizona, Tucson, AZ.

Note. Associate Editor: Samuel Easterling. Discussion open until December 1, 1997. To extend the closing date one month, a written request must be filed with the ASCE Manager of Journals. The manuscript for this paper was submitted for review and possible publication on May 22, 1995. This paper is part of the *Journal of Structural Engineering*, Vol. 123, No. 7, July, 1997. ©ASCE, ISSN 0733-9445/97/0007-0903-0911/\$4.00 + \$.50 per page. Paper No. 10784.

backing tape for handling. Fabrics are made of yarns stitched into a geometric form. The yarns may run unidirectionally like the continuous fiber sheets, or be woven at different angles into a fabric. Since there is no adhesion between individual fibers, a polymer or resin matrix is used to transmit forces between the fibers. Polymers, which include the epoxy used in this study, have the advantages of low cost, ease of workability, and some have good resistance to environmental effects. The hand, or contact layup is the oldest method of assembling an FRP. The epoxy is applied to one or both sides of the fabric and worked between the fibers using an ordinary paint roller and hand pressure. The surface may then be finished with a flexible blade to remove excess epoxy before curing occurs.

The most commonly used method of determining the properties of a composite material is the uniaxial tension test (ASTM 1993). For this test, a specimen of the FRP is instrumented either by extensometer or strain gages and placed in tension. A typical stress-strain curve for the FRP used in this study is shown in Fig. 1. The stresses in this figure were calculated based on the cross section of the composite including the polymer matrix. The tensile strength of the individual fibers is significantly higher. Note that the elastic modulus varies for different fiber orientations. When the load is applied at 0° or 90° to the fibers, the behavior is linear elastic. However, when the load is applied at an angle to the fibers, the behavior is nonlinear as shown in the figure. The stress-strain response of an off-axis ply cannot be directly computed but an approximation may be obtained by considering each ply to be orthotropic and manipulating the stiffness matrix. The elastic modulus thus computed describes the initial slope of the stress-strain curve and this is applicable for low strain values. To obtain the full curve, and determine the behavior near the ultimate strength, empirical relationships must be employed.

ANALYTICAL STUDY

An incremental deformation technique was utilized to predict the flexural behavior of the beams. The neutral axis was obtained by iteration and summation of the forces within the various components of the beam. A computer program was developed to perform the numerical analysis. The output from the program was used to plot the load versus deflection and the load versus strain behavior of the beams throughout the entire range of loading up to failure.

The Park and Paulay numerical approximation (Park and Paulay 1975) of the Hognestadt stress block was used to calculate the stress in concrete. The steel reinforcing was assumed to be elastic perfectly plastic. The FRP stress-strain response for fibers oriented along the axis of the beam or at right angle to it, was modeled as linear elastic to failure. Carbon fiber reinforced plastic (CFRP) sheets with fibers at 45° to the axis were modeled as trilinear approximations of the test results. Fig. 2 shows the idealized forces, strains, and corresponding stresses within a concrete beam resisting an applied moment. Similar to the flexural analysis of a traditionally reinforced beam, a compressive force was assumed in the concrete in the top part of the section, balanced by tensile forces in the rebar and FRP below. The contribution of the FRP sheets bonded to the web was ignored in calculating the flexural strength of the beams.

Shear strength was approximated using the American Concrete Institute (ACI) equations and modifying these equations to include the contribution of the FRP to the shear strength of the upgraded beams. The nominal strength V_n of the shear specimens in this experiment was computed from

$$V_n = V_c + V_s + V_f \quad (1)$$

where V_c and V_s are given by ACI equations 11-5 and 11-

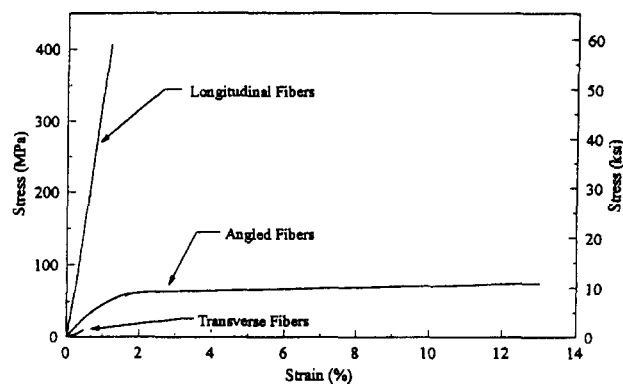


FIG. 1. Typical FRP Stress Strain Relationship for Various Fiber Orientations

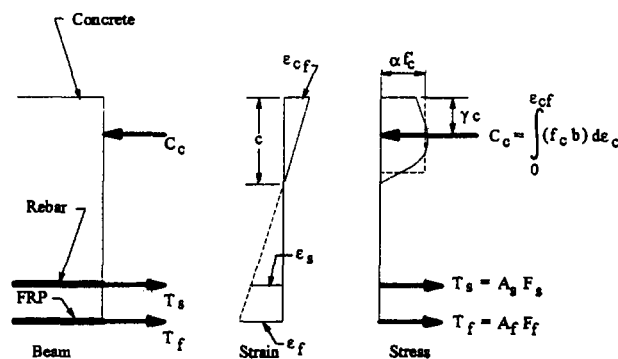


FIG. 2. Internal Forces, Strains, and Stresses in a Concrete Beam

15 (ACI 1995). The contribution of the CFRP V_f is determined by considering its strength and fiber orientation and assuming a perfect bond along the web of the beam. The CFRP applied to the web has a known thickness and its strength in any direction can be computed or determined experimentally. Assuming the maximum height for shear crack to be equal to the effective depth of the section, d , the horizontal projection of a shear crack along a 45° path is also, d . Therefore, the contribution of the CFRP sheet to the shear capacity of the beam can approximately be calculated from

$$V_f = F_{uf} t_f d \quad (2)$$

where t_f = thickness of CFRP laminate; F_{uf} = tensile strength of CFRP, in a direction parallel to stirrups; and d = distance from compression flange to centroid of tension steel. Eq. 2 applies only to a mode of failure where fibers in the composite sheet would rupture. Further studies are needed to develop equations that consider other modes of failure such as adhesive failure at the bond line or failure of concrete substrate.

EXPERIMENTAL STUDY

The experimental study consisted of casting nineteen concrete beams, precracking most of the beams, applying FRP to the tension flange and web, and loading each beam to failure. Each beam had a 5 in. × 8 in. (127 mm × 203 mm) cross section. Thirteen of the beams (flexural test specimens) were over reinforced for shear by closely spacing the stirrups. The beams were reinforced in this manner to prevent shear failure and to isolate the flexural behavior from shear behavior. The flexural reinforcement ratio $\rho = 0.0067$ used for the specimens, was close to the minimum allowed under the ACI code. These 96 in. (2,440 mm) long beams were designed to be simply supported and loaded at the quarter points to provide a region of constant moment and no shear in the center of the beam.

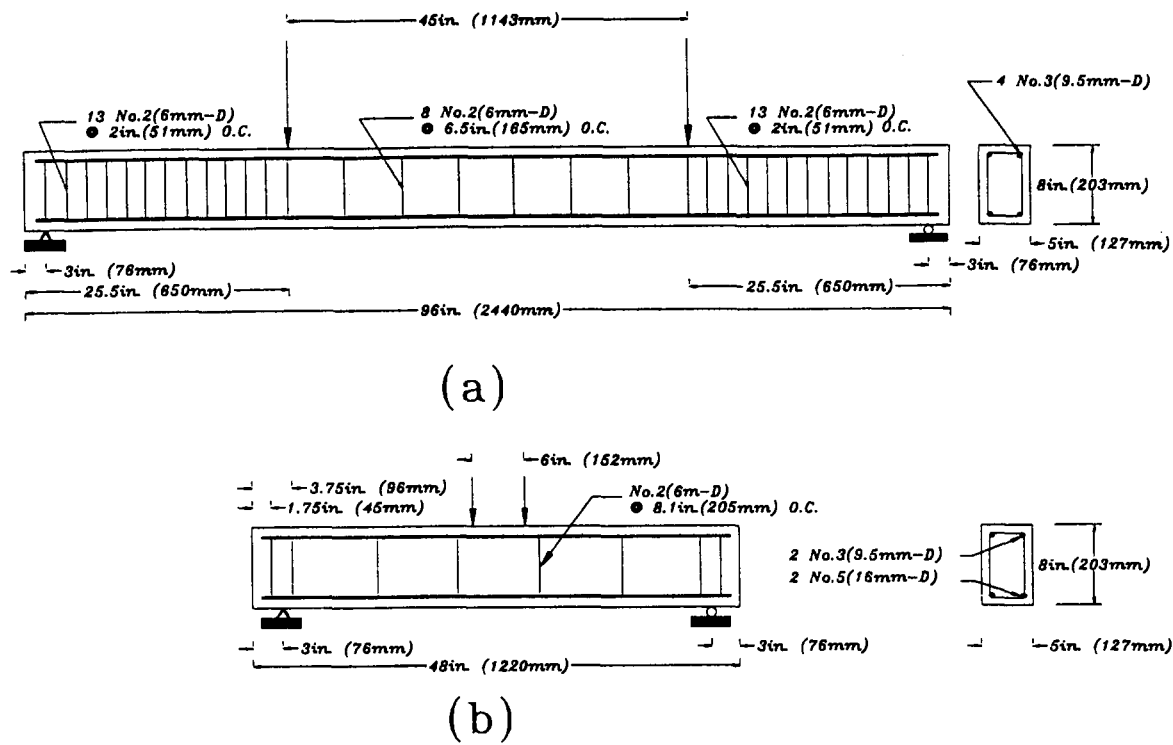


FIG. 3. Test Specimens: (a) Flexural Beams; (b) Shear Beams

TABLE 1. Test Specimens

Beam designation (1)	Flexural or shear specimen (2)	FRP system (3)	FRP orientation (see Fig. 4) (4)
C96	Flexural	(none)	(none)
C48	Shear	(none)	(none)
IA	Flexural	1	A
IB	Flexural	1	B
IBu	Flexural	1	B
IBi	Flexural	1	B
IC	Flexural	1	C
ID	Flexural	1	D
IE	Shear	1	E
IF	Shear	1	F
IIA	Flexural	2	A
IIB	Flexural	2	B
IIBu	Flexural	2	B
IIBi	Flexural	2	B
IIIC	Flexural	3	C
IIID	Flexural	3	D
IIIE	Shear	2	E
IIIF	Shear	3	F
IIIFu	Shear	3	F

The flexural reinforcement in these beams consisted of two no. 3 (9.5 mm ϕ) grade 60 tension and two no. 3 (9.5 mm ϕ) grade 60 compression bars. The spacing for the no. 2 (6 mm ϕ) stirrups in the central region of no shear was 6.5 in. (165 mm) and in the region between the supports and load points was 2 in. (51 mm). At the same time, six 48 in. (1,220 mm) long shear specimens were also cast. In these beams, the flexural reinforcement ratio was $\rho = 0.0193$. The reinforcement consisted of two no. 5 (16 mm ϕ) tension and two no. 3 (9.5 mm ϕ) compression bars. No. 2 (6 mm ϕ) stirrups were spaced at a distance of 8.1 in. (206 mm), greater than the effective depth d so shear cracks would develop easily. These shorter beams were simply supported and loaded close to the center to provide a region of constant shear over most of the beam, while developing small internal moments. Fig. 3(a) and (b)

show the reinforcement details and loading of flexural and shear specimens, respectively.

This study initially tried to isolate two sets of variables: the effect of three different fiber/epoxy systems, and several fiber orientations on the behavior of the composite beams. The test matrix also included the investigation of the effect of the composite in flexure and in shear by using the specially designed specimens described previously. Each beam was designated in a way to reflect the design variables involved in that beam. Table 1 summarizes all test specimens. A description of each variable in the beam designations is given in the following.

The control, unretrofitted beams are designated by letter C followed by either 96 or 48, indicating the length of flexural or shear specimen, respectively. I, II, and III refer to the FRP system used, and A–F refer to the fiber orientation as will be described in the subsequent sections; u designates beam uncracked before FRP was applied; and i indicates beams with additional strain gages.

Three types of FRP systems (fiber/epoxy systems) were used in the study. FRP system 1 consisted of continuous fiber sheets and a commercially available epoxy hereafter referred to as epoxy A, designed for civil engineering application. Continuous fiber sheets have a broad uniform layer of parallel fibers held in place by a paper backing, which is peeled away during installation. Two layers of fibers were used to make this system (the fiber orientations will be described) and the thickness of the composite fiber/resin matrix was approximately 0.043 in. (1 mm). FRP system 2 was made from a unidirectional fabric and a rubber toughened epoxy hereafter referred to as epoxy B. This fabric had the same parallel fibers lightly stitched together to form a cohesive product for handling prior to installation. Two layers of fabric were used for this system with a composite (fiber/resin) thickness of 0.043 in. (1 mm). FRP system 3 was composed of a cross ply fabric and the same epoxy as that for system 2. In this fabric, equal sized bundles of fibers were interwoven in two perpendicular directions. One layer of this fabric was used, resulting in a composite system thickness of .059 in. (1.5 mm). This system was used in specimens requiring fibers perpendicular to the

TABLE 2. Test Results of Fiber Reinforced Plastic (FRP) Systems

FRP system (1)	Epoxy (2)	Fiber orientation (3)	Tensile strength (ksi) (4)	E_x , longitudinal modulus (ksi) (5)	E_y , transverse modulus (ksi) (6)	E_s , shear modulus (ksi) (7)	Poisson's ratio (ν_x) (8)
1	A	0°	56.5 389.7 ^a	4.9 34.1 ^b	0.6 4.6 ^b	0.9 6.3 ^b	0.36
1	A	90°	1.6 11.3 ^a	4.9 34.1 ^b	0.6 4.6 ^b	0.9 6.3 ^b	0.36
1	A	±45°	9.8 67.8 ^a	4.9 34.1 ^b	0.6 4.6 ^b	0.9 6.3 ^b	0.36
2	B	0°	57.3 395.3 ^a	4.8 33.4 ^b	0.41 2.8 ^b	0.8 5.5 ^b	0.36
2	B	90°	2 13.8 ^a	4.8 33.4 ^b	0.41 2.8 ^b	0.8 5.5 ^b	0.36
2	B	±45°	11.3 78.2 ^a	4.8 33.4 ^b	0.41 2.8 ^b	0.8 5.5 ^b	0.36
3	B	0/90°	35.6 245.7 ^a	4.1 28.3 ^b	4.1 28.3 ^b	0.9 6.3 ^b	0.04
3	B	±45°	15.2 104.7 ^a	4.1 28.3 ^b	4.1 28.3 ^b	0.9 6.3 ^b	0.04

^aValues in MPa.

^bValues in GPa.

TABLE 3. Test Results of Epoxies

Epoxy (1)	Tensile strength (ksi) (2)	Elastic modulus (ksi) (3)	Maximum strain at failure (%) (4)
A	4.2 28.9 ^a	0.65 4.5 ^b	15.5
B	4.1 28.3 ^a	0.42 2.9 ^b	10.2

^aValues in MPa.

^bValues in GPa.

beam axis. This FRP system was thicker than the first two, because of the over/under weave of the fabric, but contained the same amount of carbon fiber per unit area of coverage as the other two systems. Tables 2 and 3 summarize the properties of the FRP systems (fiber/epoxy systems) and the properties of the epoxy itself, respectively. Each of the FRP systems was tested with respect to three fiber orientations (0°, 90°, and ±45°) except FRP system 3, which was a balanced 0/90° weave and was tested only in two orientations, 0/90° and ±45°.

Approximately the same weight of fiber was applied to each beam. The only variable in these beams was the orientation of the fibers relative to the axis of the beam and the FRP system. To simulate the conditions of a field repair, the FRP fabric was extended to within 1 in. (25 mm) of the supports. Both epoxies A and B required room temperature curing and came in two parts, mixed shortly before use into a thick liquid. All beams were sandblasted with 00 grit abrasive to prepare the surfaces. The FRP systems were applied to the surface of the beams using the hand layup method described earlier.

Fiber orientation with respect to the axis of the beam was used as a variable in these tests. Fiber orientations were designated A–D for flexural specimens and E and F for shear specimens. A sketch of these orientations is shown in Fig. 4. Fiber orientations consisted of: (A) two layers of longitudinal fibers attached to the flange and web using FRP systems 1 and 2; (B) two unidirectional layers of fibers with orientation parallel and perpendicular to the beam axis, bonded to the flange and web using FRP systems 1 and 2, where the first layer of fibers was applied along the axis of the beam and the second layer was oriented transverse to the beam axis; (C) two layers of fibers applied at ±45°, approximately normal and parallel

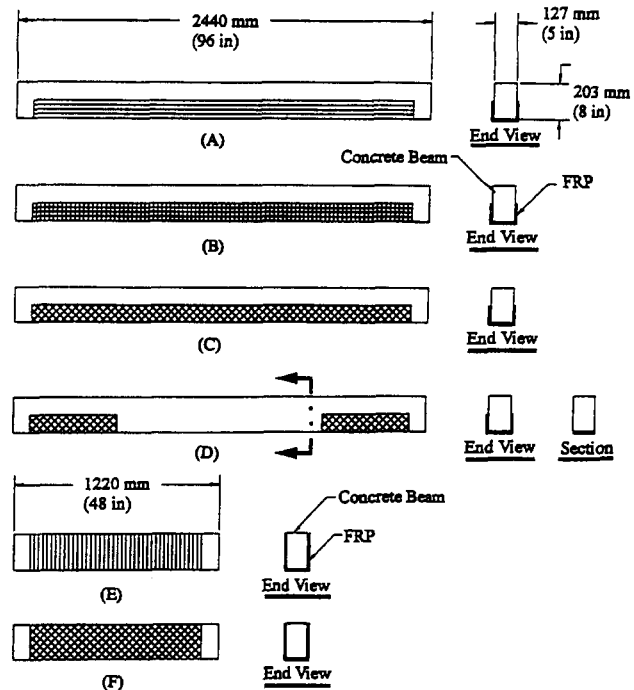


FIG. 4. Fiber Orientations A through F

to the shear cracks; (D) same as (C) except the central portion of the FRP in the region of zero shear was cut out; (E) FRP system 1 with longitudinal fibers applied perpendicular to the beam axis; and (F) same as (C) except that the FRP system covered the entire web.

Since this is a repair procedure, it was desired to apply the FRP to beams with existing cracks. Most of the specimens were preloaded to crack the concrete, yet not stress the steel reinforcement beyond yielding. Some beams were left uncracked as control specimens.

The steel rebars and concrete used for the beams were tested to determine their strength. The steel had an average yield stress of 61,000 psi (420 MPa), and the concrete had an average compressive strength of 5,300 psi (36.5 MPa) at the time the beams were tested.

TEST RESULTS

There was little difference between the various forms of fibers used; the continuous fiber sheets behaved much like the

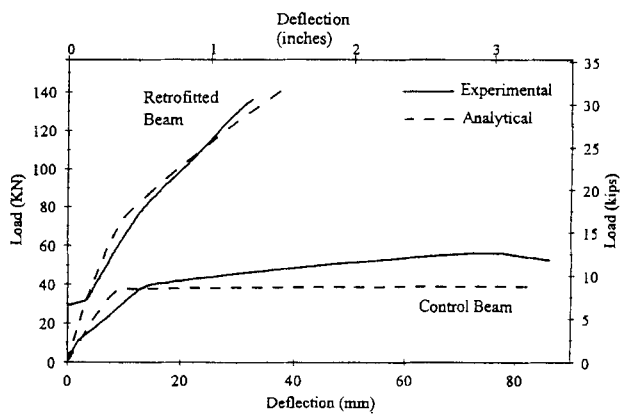


FIG. 5. Beam IA: (a) Load versus Deflection; (b) at Failure

stitched or woven fabrics. However, because of the paper backing, used with the stitched and woven fabrics, installation of the continuous fiber sheets was somewhat simpler. There was no difference in behavior between the precracked beams and the uncracked ones at the ultimate level. The most significant differences were due to various fiber orientations and web coverages. These corroborated earlier studies for fibers oriented longitudinally (Saadatmanesh and Ehsani 1990; Saadatmanesh and Ehsani 1991), and showed new possibilities for field applications of diagonal plies. The behavior of a typical beam from each fiber orientation is described here and its mode of failure discussed.

FLEXURAL SPECIMENS

Beam IA had the fibers oriented longitudinally on both the tension flange and web. The load deflection relationship for this beam is shown in Fig. 5(a). It appears that some measurement error was encountered in reading the deflection at the initial stages of loading, since no measurable deflection was recorded up to a load of 7 kips (31 kN). Also shown, are similar plots for the control beam C96 and the predicted results. The predicted results were obtained using the procedures outlined in a paper by An et al. (1991). A computer program was developed to generate the load-displacement and the load-strain curves throughout the entire range of loading up to failure. The computer program predicted with reasonable accuracy the increase in stiffness and ultimate strength due to the composite action of FRP and concrete beam. The sudden change in the slope of the curves for the control beam shows the point at which the stress in the tension rebars exceeded yield stress σ_y . This effect was less pronounced in the retrofitted beam. By comparing the retrofitted beam with the control beam, it can be seen that the load at which the steel yielded was higher for the retrofitted beam, suggesting that the internal forces were shared between the carbon fibers and the steel. In addition, the retrofitted beam showed greater ultimate strength

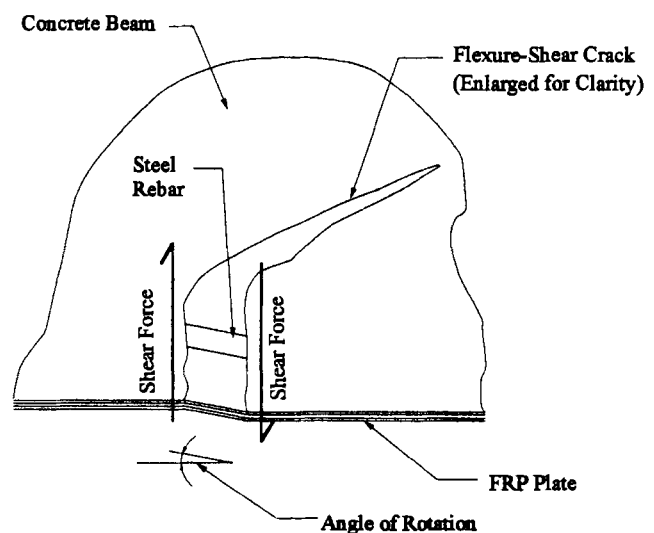


FIG. 6. Mechanism of FRP Plate Delamination

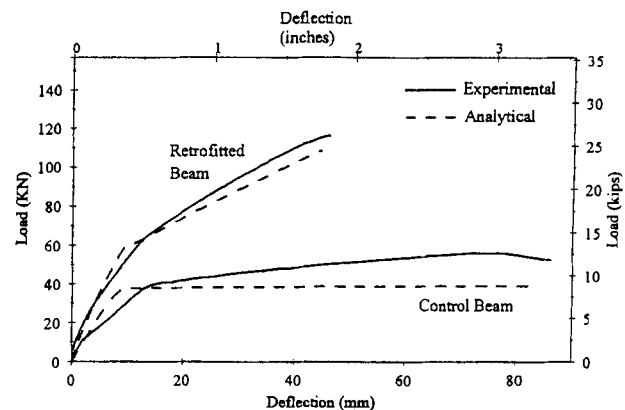


FIG. 7. Beam IB: (a) Load versus Deflection; (b) at Failure

than the control beam as loading increased to 31 kips (138 kN) before the beam abruptly failed. This was due to the peeling of the CFRP laminate from the concrete. As a result of stress concentration at the plate end, the concrete rupture strength was exceeded at this point and a crack formed just outside the repaired area. This crack propagated quickly in the tension face of the beam toward the load point destroying the beam as shown in Fig. 5(b). The fatal crack propagated in three dimensions tearing a diagonal piece out of the web in the region of constant shear between the load and the support. The CFRP separated from both the web and tension face over about half the length of the beam. This type of failure, that is separation of plate in conjunction with part of the substrate (concrete) could also occur in the vicinity of flexure-shear

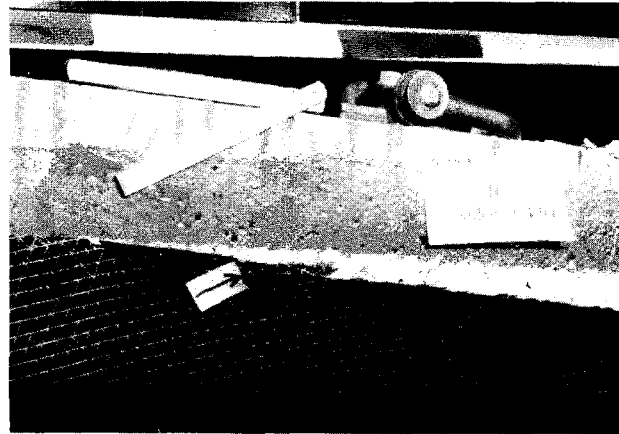
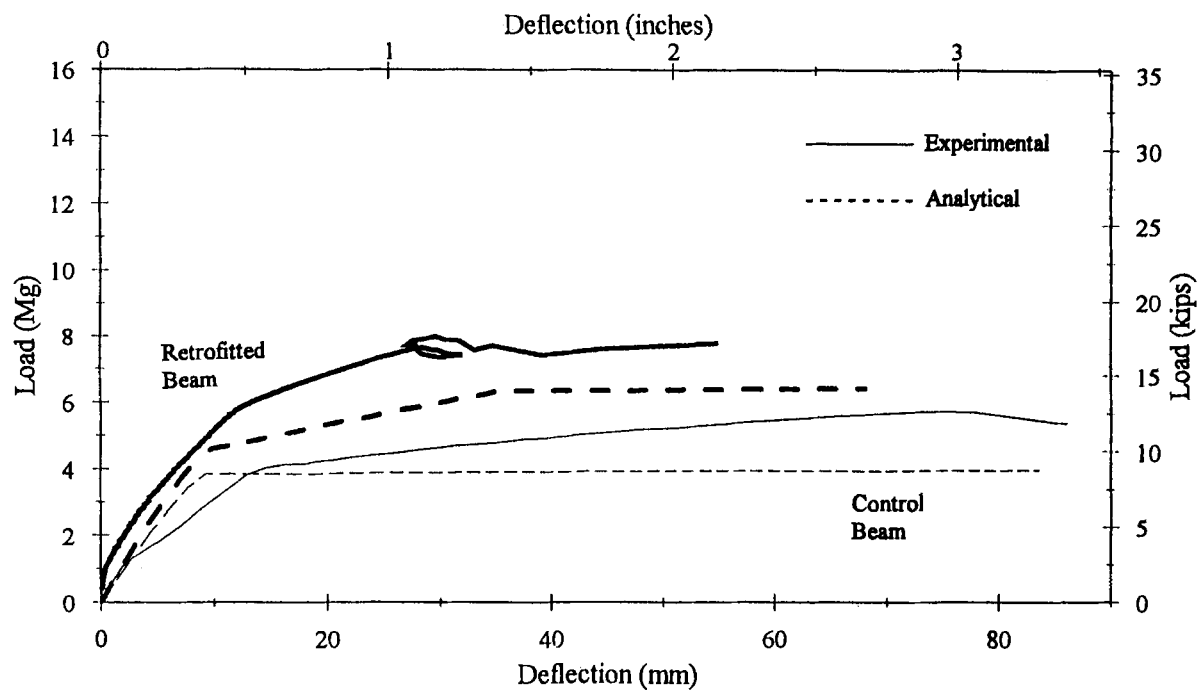


FIG. 8. Beam IC: (a) Load versus Deflection; (b) at Failure

cracks, as is graphically shown in Fig. 6 and was observed in other experiments (Saadatmanesh and Ehsani 1991).

Beam IB was representative of the behavior of the $[0^\circ/90^\circ]$ cross ply layup. The load deflection plot is shown for this and the control beam in Fig. 7(a) along with the analytical results. In this beam, only half of the fibers were used in the longitudinal direction, and therefore, the ultimate strength is less than that of beam IA. Still it is a significant improvement over the control beam. The composite action of the CFRP and the concrete beam noted for the previous beam can also be seen here in the form of elevated steel yield load. For fiber orientation B, the beams failed differently. The beams that were loaded rapidly, experienced concrete failure at the end of the CFRP similar to those beams with the longitudinal fibers. Those that were loaded slowly, failed below one of the loading points by tensile failure of the CFRP fibers. Two of the fiber orientation B beams (IBi and IIBi) were fitted with several additional FRP strain gauges, both along the tension face and web. This instrumentation indicated that new flexural cracks began to occur closer to the termination points of the CFRP laminate as moments progressively increased and stresses in the longitudinal fibers were transferred up the web through the transverse ply. The ultimate load of the test specimen was close to that predicted by the analysis for beam IIB. This varied slightly for other beams with this fiber orientation, but in

all cases these beams failed less explosively than the beams with longitudinal fibers alone. The CFRP did not split apart and separate from the webs and flange in three directions, but held together after failure, as shown in Fig. 7(b). The concrete between the tension steel and the CFRP failed, but it was all contained by the CFRP shell. Separation occurred on the tension flange as well as the web, indicating that stresses were transferred to the surface of the web by the transverse fibers, as was indicated by strain readings from the additional gauges placed on the web.

Beam IC had the fibers applied at $\pm 45^\circ$ to the axis of the beam. As predicted by the computer analysis, the beam showed less increase in strength and stiffness as compared to those beams with longitudinal fibers. The load deflection plots for experimental and predicted responses are shown in Fig. 8(a). The overall behavior of this beam was more ductile than the first two beams. The failure mode of this beam was also significantly different than the first two; it occurred slowly in a ductile manner. As deflection increased, the top edge of the CFRP began to separate from the web [see Fig. 8(b)] and loading was stopped.

Beams with fiber orientation D had $\pm 45^\circ$ FRP fibers applied like beams with fiber orientation C but the web reinforcing was cut away in the midspan region of low shear. This resulted in a smaller development length of the fibers near the center

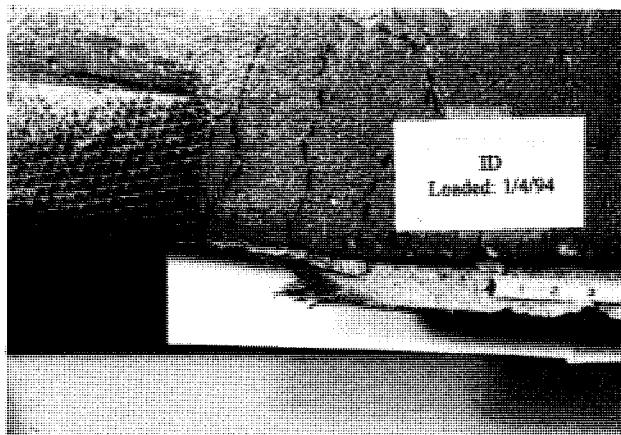
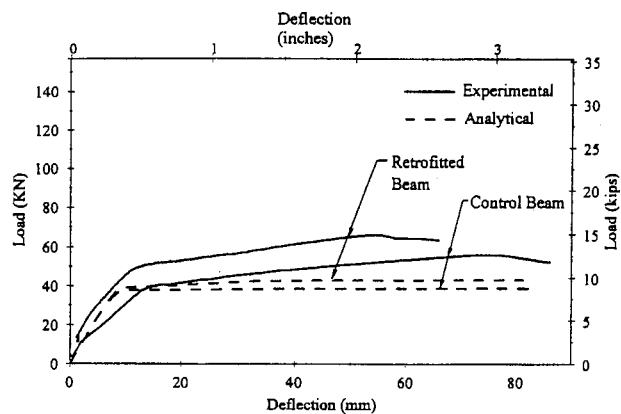


FIG. 9. Beam ID: (a) Load versus Deflection; (b) at Failure

of the beam. That is, fibers bonded to the tension flange began at one side of the flange, crossed it diagonally, and ended at the other side of the flange. Because of this, the beam was the least improved of all the flexural specimens, as shown in the load displacement curve of beam ID in Fig. 9(a). Some increase in flexural stiffness is seen and this beam exhibited a ductile, gradual failure like beam IC described earlier. Loading was stopped when the deflection became excessive, and upon unloading, it was discovered that the CFRP had separated from the concrete along the interface. The actual CFRP failure varied between the two beams with this fiber orientation (ID and IIID). Beam ID was reinforced with FRP system 1; a ply of continuous fiber sheet was bonded to the beam at 45° and then covered with a second perpendicular layer. As the CFRP failed, the outer layer displaced laterally exposing the ends of the ruptured fibers, as shown in Fig. 9(b). Beam IIID was retrofitted with FRP system 3. The woven cross ply fabric was bonded at 45° to the axis of the beam. In this orientation, the fabric itself had little longitudinal strength and any increase in strength is probably due to factors other than the fabric.

SHEAR SPECIMENS

The behavior of CFRP composite shear specimens retrofitted with transverse fibers is shown by beams IE and IIE. These beams received fiber orientation E, with fibers wrapped around the tension face and up to the full height of the web to simulate the action of steel stirrups. These beams were overreinforced for flexure, $\rho > \rho_{max}$, and no longitudinal CFRP fibers were used. The load deflection plot for beam IE is shown in Fig. 10(a) along with that of the shear control beam, C48. The control beam failed in shear, as is evident by a lack of a distinct yield point on the load-deflection response. Fig. 10(b) shows the control beam at failure. The load-deflection relationship for this beam was not predicted, instead, the ultimate

shear strength was computed using the approximate formula developed in the section on analysis for shear and this strength is shown on the plot by a horizontal line. As expected, the FRP increased the shear strength of the beam. In fact, it was increased to the point that shear failure never actually occurred in the retrofitted beam. Rather, loading was halted when the beam failed due to tension steel yielding and separation of the CFRP fibers from concrete near midspan. This is shown in Fig. 10(c). The behavior of beam IIE was similar to IE. Strain gauges on the web and tension flange of this beam showed elongation of transverse FRP prior to failure, indicating effectiveness of the CFRP in resisting shear. A load strain plot is shown in Fig. 10(d) for beam IIE. The direction of the fibers are shown on the inset sketch as well as the location of two strain gauges (FRP3 and FRP5) halfway to the top of the beam. As loading increased, CFRP strain recorded by these

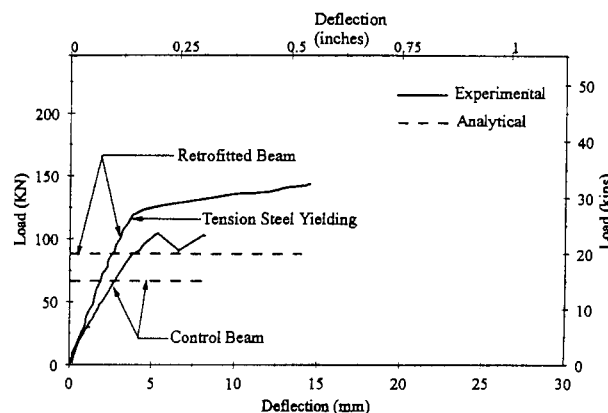


FIG. 10(a). Beam IE: Load versus Deflection

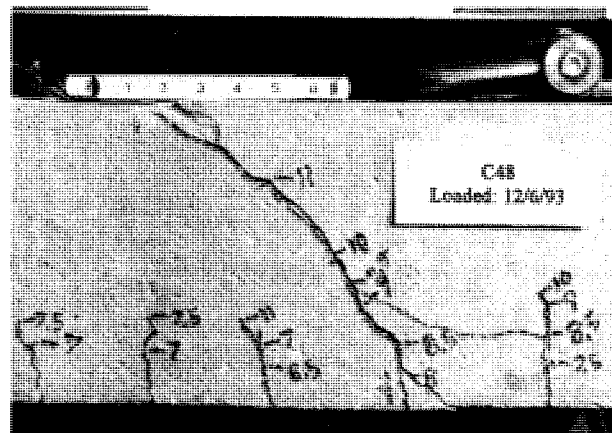


FIG. 10(b). Control Shear Beam at Failure

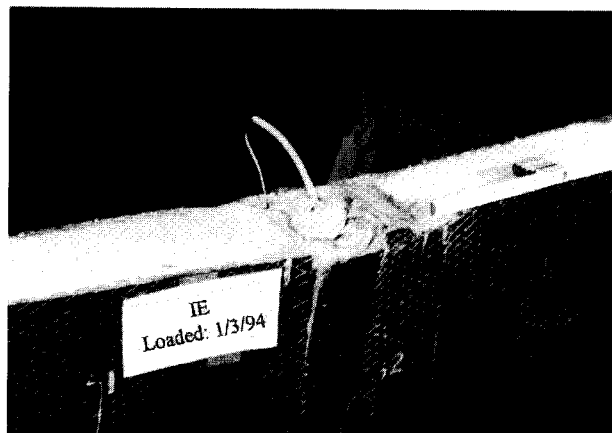


FIG. 10(c). Beam IE at Failure

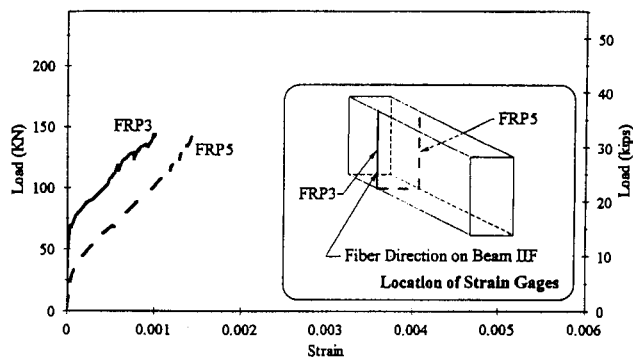


FIG. 10(d). Beam IIE: Load versus CFRP Strain at Web

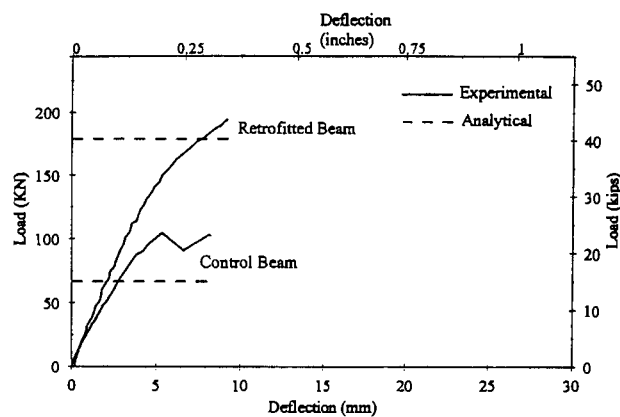
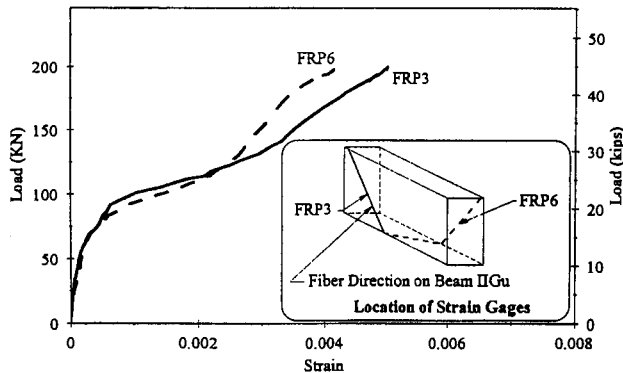


FIG. 11. Beam III Fu: (a) Load versus CFRP Strain at Web; (b) Load versus Deflection; (c) at Failure

gauges increased abruptly indicating the formation and widening of shear cracks in the concrete beneath, and resistance developed in the CFRP sheet for carrying portion of the shear.

A similar plot is shown in Fig. 11(a) for beam III Fu. This beam was uncracked prior to application of the CFRP using

fiber orientation F. In this orientation, CFRP fibers were placed at 45° to the axis of the beam and covered the web of the beam on both sides. It can be seen by the strain in the CFRP that the diagonal shear cracks formed and widened as load increased. The reverse curvature shown in the plot as loading exceeded 25 kips (125 kN) is probably due to redistribution of forces in the cross ply fibers. As with orientation A of the flexural series, that provided fiber orientation perpendicular to flexural cracks, fiber orientation F provided CFRP fibers normal to the diagonal shear cracks. The load deflection plot for this beam and the corresponding control beam are shown in Fig. 11(b). As expected, the ultimate strength of this beam exceeded that of IE; however, this beam was stiffer than beam IE and it failed more abruptly than IE. In the case of beam III Fu, the fatal crack occurred at the end of the FRP at the top; the anchorage point for the most highly stressed fibers. Fig. 11(c) shows that the concrete ruptured at the top face of the beam as the end of the CFRP peeled away.

Figs. 12 and 13 show the range of improvement provided by the CFRP retrofit in the flexural groups and shear groups, respectively. An increase in strength and stiffness was seen in every specimen to which CFRP was applied, regardless of the fiber orientation. There was also a direct correlation seen consistently between the magnitude of the increase and the brittleness of the failure. In both shear and flexural specimens, when the fibers were placed perpendicular to cracks in the beam, the result was higher stiffness and with brittle failure caused by concrete rupture in a place unique to this application. This included fibers placed longitudinally across flexural cracks or normal to diagonal shear cracks. Where double CFRP layers were used, the fibers placed transverse to the first layer tended to contain the fractured concrete, but the rupture was still abrupt because of those fibers perpendicular to the cracks. When fibers were placed obliquely to the cracks, the

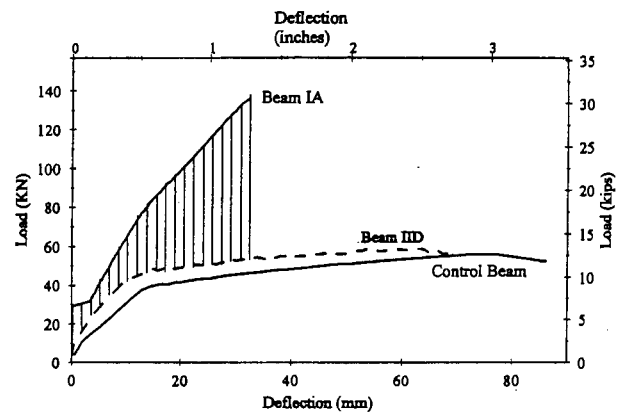


FIG. 12. Improvement Envelope—Flexural Beams

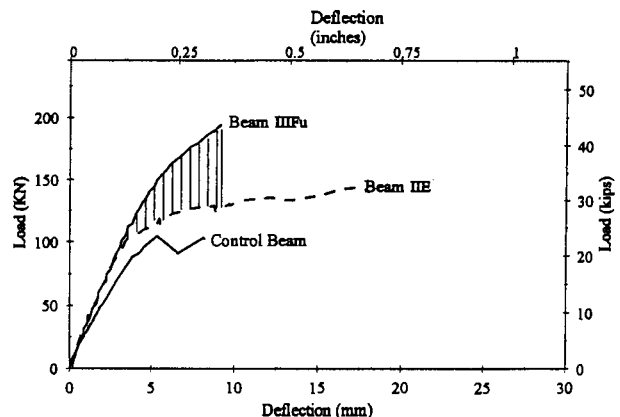


FIG. 13. Improvement Envelope—Shear Beams

increase in stiffness was less and the mode of failure was ductile. This was seen with $\pm 45^\circ$ fibers crossing flexural cracks and fibers placed vertically on the web across diagonal shear cracks. It was also noted that the magnitude of the increase was directly related to the development length of the fibers on both sides of the cracks.

CONCLUSIONS

CFRP sheets can provide increase in strength and stiffness to existing concrete beams when bonded to the web and tension face. The magnitude of the increase and the mode of failure are related to the direction of the reinforcing fibers. When the CFRP fibers were placed perpendicular to cracks in the beam, a large increase in stiffness and strength was observed and a brittle failure occurred due to concrete rupture as a result of stress concentration near the ends of the CFRP. This was true whether flexural or shear cracks in the beam were repaired. When the CFRP fibers were placed obliquely to the cracks in the beam, a smaller increase in strength and stiffness was observed; however, the mode of failure associated with this off-axis application of CFRP was more ductile and preceded by warning signs such as snapping sounds or peeling of the CFRP. The micromechanics of an off axis CFRP failure are an emerging study and need to be investigated more fully before this phenomenon can be completely understood. Yet the results of this study show that CFRP may be used to increase the strength and stiffness of beams without causing catastrophic brittle failures associated with this strengthening technique, certain combination of fibers and orientations may provide the ductile yielding properties of steel plate retrofits without the interface corrosion problems noted in earlier field applications with bonded steel plates.

ACKNOWLEDGMENTS

The writers would like to acknowledge the contribution of the Federal Highway Administration and funding by the National Highway Institute and staff of the Turner Fairbank Highway Research Center in McLean, Va. Additional funding was received from the National Science Foundation, under grant No. MSS-9257344. The writers would like to thank Eric Munley and John B. Scalzi.

APPENDIX I. REFERENCES

- American Concrete Institute (ACI). (1995). "Building code requirements for reinforced concrete and commentary." *ACI 318-95*, Detroit, Mich.
- An, W., Saadatmanesh, H., and Ehsani, M. R. (1991). "RC beams strengthened with GFRP plates II: analytical and parametric study." *J. Struct. Engrg.*, ASCE, 117(11), 3434-3455.
- Dolan, C. W., Rider, W., Chajes, M. J., and DeAscanis, M. (1993). "Pre-stressed concrete beams using non-metallic tendons and external shear reinforcing." *Proc., Int. Symp. on Fiber-Reinforced-Plastic Reinforcement for Concrete Struct.*, Am. Concrete Inst., 138, 475-495.
- Dusseck, I. (1987). "Strengthening of bridge beams and similar structures

- by means of epoxy-resin-bonded external reinforcement." *Transp. Res. Rec. No. 785*, Transp. Res. Board, Washington, D.C., 21-24.
- Federal Highway Administration (FHWA). (1993). "Highway bridge replacement and rehabilitation program." *11th Rep. of the Secretary of Transp. to the Congress of the United States*, Bridge Div., Ofc. of Engrg., Washington, D.C.
- Klaiber, F. W., Dunker, K. F., Wipf, T. J., and Sanders, W. W. (1987). "Methods of strengthening existing highway bridges." *Nat. Cooperative Hwy. Res. Program Rep. No. 293*, Transp. Res. Board, Washington, D.C.
- Meier, U., and Kaiser, H. P. (1991). "Strengthening of structures with CFRP laminates." *Proc., Conf. on Advanced Compos. Mat. in Civ. Engrg. Struct.*, ASCE, 224-232.
- Park, R., and Paulay, T. (1975). *Reinforced concrete structures*. John Wiley & Sons, Inc., New York, N.Y.
- Ritchie, P., Thomas, D., Lu, L., and Connelly, G. (1990). "External reinforcement of concrete beams using fiber reinforced plastics." *ATLSS Rep. No. 90-06*, Lehigh Univ., Bethlehem, Pa.
- Rostasy, F. S., Hankers, C., and Ranish, E. H. (1991). "Strengthening of R/C and P/C structures with bonded FRP plates." *Proc., Conf. on Adv. Compos. Mat. in Civ. Engrg. Struct.*, ASCE, New York, N.Y., 253-263.
- Saadatmanesh, H., and Ehsani, M. R. (1990). "Fiber composite plates can strengthen beams." *Concrete Int.*, (Mar.), 65-71.
- Saadatmanesh, H., and Ehsani, M. R. (1991). "RC beams strengthened with GFRP plates I: experimental study." *J. Struct. Engrg.*, 117(11), 3417-3433.
- Sakai, K., Uchida, Y., Okamoto, J., Yoshita, H., and Komatsu, K. (1992). "Flexural performance of a steel reinforced concrete beam reinforced with carbon sheet." *Proc., 47th Meeting of the Japan Soc. of Civ. Engrs.*
- Standard test method for tensile properties of fiber-resin composites: D3039/D3039M-93*. (1993). West Conshohocken, Pa., 119-127.
- Triantafyllou, T., and Plevris, N. (1991). "Post strengthening of R/C beams with epoxy bonded fiber composite materials." *Proc., Conf. on Advanced Compos. Mat. in Civ. Engrg. Struct.*, ASCE, New York, N.Y., 245-256.
- Uji, K. (1992). "Improving shear capacity of existing reinforced concrete members by applying carbon fiber sheets." *Trans. of the Japan Concrete Inst.*, Vol. 14, 253-265.

APPENDIX II. NOTATION

The following symbols are used in this paper:

- d = effective depth;
 f = ultimate tensile strength;
 t = thickness;
 V = shear strength; and
 σ = stress.

Subscripts

- c = concrete;
 f = fiber composite;
 n = nominal;
 s = steel;
 uf = ultimate strength of fibers; and
 y = yield.